Superfine Structure, Physical Properties, and Dyeability of Alkaline Hydrolyzed Poly(ethylene terephthalate)/Silica Nanocomposite Fibers Prepared by *In Situ* Polymerization

Yongzhe Yang, Hongchen Gu

National Key Laboratory of Nano/Micro Fabrication Technology, Key Laboratory for Thin Film and Microfabrication of Ministry of Education, Institute of Micro and Nano Science and Technology, Shanghai Jiaotong University, Shanghai 200030, China

Received 18 January 2006; accepted 22 February 2006
DOI 10.1002/app.24268
Published online in Wiley InterScience (www.interscience.wiley.com).

ABSTRACT: In this study, poly(ethylene terephthalate) (PET)/SiO_2 nanocomposites were synthesized by *in situ* polymerization and melt-spun to fibers. The superfine structure, physical properties, and dyeability of alkaline hydrolyzed PET/SiO_2 nanocomposite fibers were studied. According to the TEM, SiO_2 nanoparticles were well dispersed in the PET matrix at a size level of 10–20 nm. PET/SiO_2 nanocomposite fibers were treated with aqueous solution of sodium hydroxide and cetyltrimethyl ammonium bromide at 100°C for different time. The differences in the alkaline hydrolysis mechanism between pure PET and PET/SiO_2 nanocomposite fibers were preliminarily investigated, which were evaluated in terms of the weight loss, tensile strength, specific surface area, as well as disperse dye uptake. PET/SiO_2 nanocomposite fibers showed a greater degree of weight loss as compared with that of pure PET fibers. More and tougher superfine structures, such as cracks, craters, and cavities, were introduced, which would facilitate the certain application like deep dyeing. © 2006 Wiley Periodicals, Inc. J Appl Polym Sci 102: 3691–3697, 2006

Key words: alkaline hydrolysis; nanocomposite; fibers; poly (ethylene terephthalate); silica

INTRODUCTION

Poly(ethylene terephthalate) (PET) commonly used for textile application represents the largest percentage among synthetic fibers in the market, and is used as pure material or mixed with cellulose. PET fiber has the most compact and crystalline structure, and is markedly hydrophobic. Its hydrophobic nature accounting for inability to wick moisture away from the body and poor launderability can be a disadvantage for its underlying applications.[1–5] To change this passive and lazy role of PET, surface modification of PET fiber without loss of bulk properties has been an oft-sought goal in the fiber industry.

One interesting chemical treatment is alkaline hydrolysis with sodium hydroxide (NaOH). Alkaline hydrolysis of PET fiber is a highly developed finishing process.[6] In theory, PET undergoes a nucleophilic substitution and is hydrolyzed by a NaOH solution. Chain scission occurs and results in considerable weight loss (WL) and hydroxyl and carboxylate end group formation so as to improve handle, soil-release properties, moisture regain, and drape of fabrics.[7–12] However, alkaline hydrolysis is only a surface and local reaction resulting in only a small change in the corresponding molecular weight, density, and crystallization.[6,13] Many variables of the alkaline hydrolysis have been studied, including fiber additives.[14–16] Solbrig et al. reported that micro-TiO_2 delusterant had been implicated in some of the changes taking place in PET fibers upon hydrolysis, notably the surface morphology.[17] Collins et al. found that greater strength loss with decreasing weight occurred and larger pits formed on the surface of fibers for the hydrolyzed PET/TiO_2 fibers than for the pure PET samples.[18]

The changes in properties of hydrolyzed PET fibers modified by nanoparticles have received little attention in the literatures. In this study, we have prepared PET/SiO_2 nanocomposites by *in situ* polymerization and melt-spun to fibers. The structural, mechanical, and dyeable properties as well as the kinetic behavior of

Correspondence to: H. Gu (hcgu@sjtu.edu.cn).
Contract grant sponsor: Key Science-Technology Project of the National ''Tenth Five-Year-Plan'' of State Development Planning Commission of China; contract grant numbers: 2001BA310A10.
Contract grant sponsor: Shanghai Nano Technology Project of China; contract grant numbers: 0213nm002, 0352nm023.

TABLE I
Fundamental Properties of Pure PET and its Nanocomposites

Specimen	Intrinsic viscosity (dL/g)	—COOH (mol/10^3 kg)	Lucency	B
Pure PET	0.68	15.3	86.2	1.4
PET/0.1 wt % SiO_2	0.69	14.1	90.6	1.2
PET/0.5 wt % SiO_2	0.68	14.8	86.5	1.6
PET/2.0 wt % SiO_2	0.68	15.6	83.4	1.5

alkaline hydrolysis for PET/SiO_2 nanocomposite fibers were thoroughly studied.

EXPERIMENTAL

Materials

Nano-SiO_2 with average particle size of 10 nm was supplied by Yuda Chemical (Zhejiang, China). Ethylene glycol (EG), terephthalic acid, trimethyl phosphate, Sb_2O_3 (as catalyst), NaOH, cetyltrimethyl ammonium bromide, and organosilane coupling agent A-187 were supplied by Chemical Reagents (China).

Preparation of the SiO_2/EG sol

Organosilane coupling agent A-187 (2.4 g) was dissolved in 100 mL water and heated at 60–70°C for 20 min. The solution was added dropwise to 100 g 25 wt % SiO_2/H_2O sol, maintaining the flow rate at 10 mL/min. Then the modified SiO_2 was transferred from water to EG by rotatory evaporation. The dispersion of 25 g of modified SiO_2 in a 100 mL of EG solution was added to another 100 mL of EG, which was heated at 80–120°C. Similarly, the flow rate was controlled at 10 mL/min. The mixture was stirred vigorously for 30 min.

Preparation of PET/SiO_2 nanocomposites by *in situ* polymerization

PET pellets with various content of SiO_2 were prepared by the PTA route. In a 5-L cylindrical reactor, 1 kg of EG (16.1 mol) and varied content of SiO_2 were placed; the mixture was stirred for 0.5 h at room temperature. Then 2 kg of terephthalic acid (12.0 mol), a few drops of trimethyl phosphate, and some Sb_2O_3 were added, with vigorous stirring to obtain a homogeneously dispersed system. The mixture was then heated in nitrogen atmosphere from room temperature to 250–260°C under a pressure of 0.3 MPa. After completed esterification, the pressure was reduced to air pressure to emit the water generated during the esterification. Then the polymerization was carried on at 260–270°C under a pressure of 200–300 Pa to remove the excess EG. Afterward, the pressure was controlled to less than 40 Pa. After 1–2 h polycondensation, the melting polymer was extruded through an orifice at nitrogen pressure of 0.3 MPa and cooled with water.

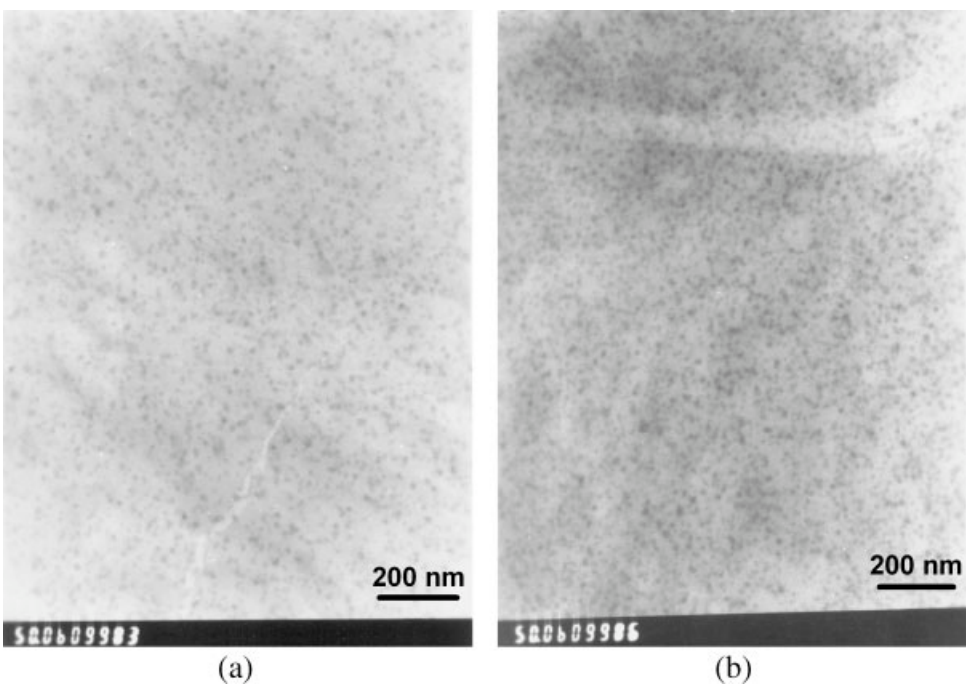

Figure 1 TEM photographs of PET/SiO_2 nanocomposites (a) 0.5 wt % SiO_2; (b) 2.0 wt % SiO_2.

TABLE II
Weight Loss of PET/SiO_2 Fibers at Different Hydrolysis Time

Sample	Weight loss (%)					
	10 (min)	20 (min)	30 (min)	40 (min)	50 (min)	60 (min)
Pure PET	13.6	25.0	31.8	41.1	45.1	49.8
PET/0.1 wt % SiO_2	14.1	25.3	33.6	41.3	45.3	51.2
PET/0.5 wt % SiO_2	14.9	25.8	34.1	41.7	45.9	54.2
PET/2.0 wt % SiO_2	16.3	26.7	34.8	49.2	57.9	61.6

Melt spinning

PET/SiO_2 pellets were subjected to melt spinning using a spinning instrument ABE-25 equipped with a spinneret with 36 nozzles of 0.3 mm diameter. The temperatures of screw extruder were set as 285, 295, 300, and 300°C, respectively. The drawing of the fibers was carried out on a Barmag 3013 drawing device with draw ratio 3.7.

Characterization

PET/SiO_2 nanocomposite specimens were sliced at −80°C with an Ultracut Uct microtome. A transmission electron microscope operated at 75 kV was used to obtain images of the specimens, which were annealed in a vacuum oven at 200°C for 1 week to remove moisture completely.

Tensile properties of PET/SiO_2 nanocomposite fibers were measured using an AGS material testing machine with gauge length of 250 mm at a crosshead speed of 500 mm/min. The elongation at break and tensile strength were obtained by averaging at least 10 trials of the tensile test for each sample.

Alkaline (NaOH) hydrolysis was performed in one bath (100°C) with the catalyst (cetyltrimethyl ammonium bromide). A soup washing (85°C) and then warm water washing, dilute acetic acid washing, and cold water washing were performed until the fibers were in a neutral situation. WL of the fibers was calculated as follows:

$$WL(\%) = [(W_0 - W_1)/W_0] \times 100$$

where W_0 and W_1 are fiber weights before and after hydrolysis, respectively.

Surfaces of alkaline hydrolyzed fibers were observed with a JEOL JSM-6340F field emission scanning electron microscopy.

Surface area and mean pore size were measured in a Pyrex holder. A 1-g sample was placed in a Pyrex holder, preheated to 100°C and outgassed to a final vacuum of 10^{-5} Torr. The full sorption (adsorption and desorption) was preformed using nitrogen at the normal boiling point of liquid nitrogen (−196°C). Surface areas were calculated using the BET equation. Pore size were obtained using nitrogen desorption.

The samples were dyed with 5% of the weight of the fibers of Disperse Blue (Foron Blue RD-S) at a liquor ratio of 1 : 100. The samples were introduced into the dye bath at 60°C, then the temperature was gradually raised up to boiling point within 20 min, and then dyeing was continued for 30 min with stirring. The dyed samples were rinsed with cold water, then soaped with a solution contained no-ionic detergent (2 g/L), at 98°C for 15 min, and rinsed with tap water. The amounts of Disperse Blue taken up by the fiber were determined from the difference between the final and initial concentration of this compound in solution, provided that adsorption equilibrium was already attained. A Hitachi model U-2000 spectrophotometer was used for the determination of dye in the solution, the maximum absorbance being 565 nm.

RESULTS AND DISCUSSION

The fundamental properties of PET/SiO_2 nanocomposites

The fundamental properties (intrinsic viscosity, carboxylate end group concentration, lucency, color parameter) of pure PET and its nanocomposites are listed in Table I. The intrinsic viscosities of the samples are approximately equal because the polymerizations were controlled by melt viscosities. It can be found from

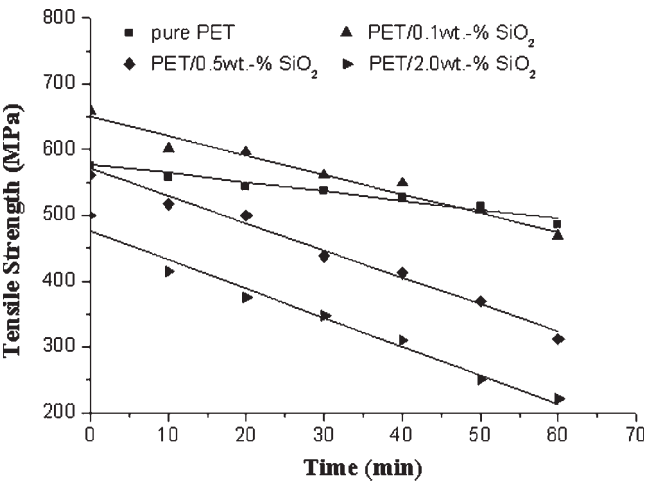

Figure 2 Tensile strength of PET fibers at different alkaline hydrolysis time.

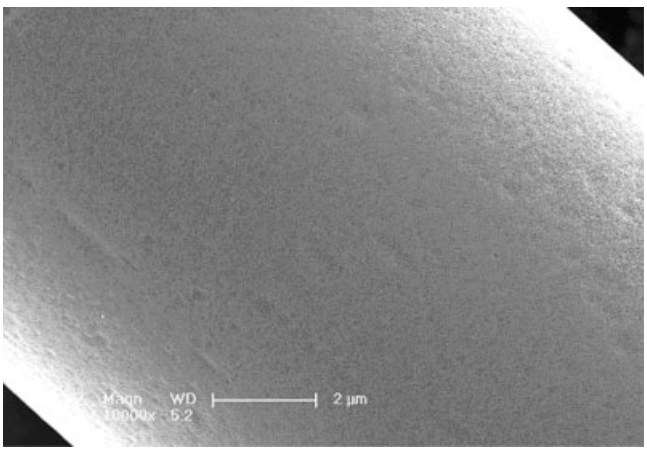

Figure 3 SEM photos of pure PET fiber alkaline hydrolyzed for 30 min.

Table I that the other parameters of PET/SiO_2 nanocomposites are also consistent with those of pure PET, which means that the introduction of SiO_2 nanoparticles has no significant effect on the polymerization process.

The dispersion of SiO_2 nanoparticles in PET matrix

It is well known that the dispersion of nanoparticles in the polymer matrix has a significant impact on the properties of composites.[19–22] As the nanoparticles have a strong tendency to agglomerate, homogeneous dispersion of the nanoparticles in the polymer has been considered as a difficult process. A good dispersion may be achieved by surface modification of the nanoparticles under an appropriate processing condition.[23] In this work, a novel approach has been utilized to disperse nanoparticles in the PET matrix. Figure 1 shows TEM images of PET-based nanocomposites having 0.5 and 2.0 wt % of SiO_2 nanoparticles, where the dark areas represent the SiO_2 nanoparticles and gray/white areas represent the PET matrix. It is clearly seen that SiO_2 nanoparticles have been dispersed fairly well. The sizes of SiO_2 nanoparticles range between 10 and 20 nm.

Alkaline hydrolysis mechanism of PET/SiO_2 nanocomposite fibers

One of the main effects of alkaline hydrolysis is WL from the PET substrate. The effect of the treatment time on WL of PET fibers from alkaline hydrolysis is given in Table II. Some authors assumed linear time dependence of WL, whereas others found an exponential function to better fit the experimental data.[9,24–26] In this study, we observed that WL increased nonlinearly with hydrolysis time. For the pure PET fiber, the relationship between %WL and time (t) can be expressed as $\%WL = 3.24 \times t^{0.67}$ (correlation coefficient $R^2 = 0.995$). In contrast, for its nanocomposite fibers, the regression equations are $\%WL = 3.41 \times t^{0.66}$ ($R^2 = 0.996$), $\%WL = 3.29 \times t^{0.68}$ ($R^2 = 0.998$), and $\%WL = 2.67 \times t^{0.78}$ ($R^2 = 0.992$) at SiO_2 content of 0.1, 0.5, and 2.0 wt %, respectively. The nonlinearity of the relation between WL and time may be attributed to the reduced —OH concentration.[27]

The rate of hydrolysis increased in the order pure PET < PET/0.1 wt % SiO_2 < PET/0.5 wt % SiO_2 < PET/2.0 wt % SiO_2, pure PET showing slowest loss in weight during the whole treatment process. WL of PET/2.0 wt % SiO_2 was almost the same as that of PET/0.1 wt % SiO_2 or PET/0.5 wt % SiO_2 initially but later (after 30 min) increased rapidly, as a result of exposing more inner weak points formed within 30-min treatment.

Mechanical properties

Addition of SiO_2 nanoparticles in the PET fibers has an influence on the mechanical properties, as shown in Figure 2. It can be seen that the effect of SiO_2 nanoparticles on the tensile strength of fibers is very distinct and the composition dependence is pronounced. Without alkaline hydrolysis, the tensile strength of PET/0.1 wt % SiO_2 fibers has a value of 659 MPa, which is 15% higher than that of pure PET fiber (575 MPa). A small addition of SiO_2 nanoparticles resulted in an obvious increase in the tensile strength, owing to a strong interaction between the SiO_2 nanoparticles and PET working as crosslinked points. These similar physical crosslinked points made the molecular network more complete and effectively enhanced mechanical properties.[28–30] However, a gradual declination in the tensile strength is observed after that and can be ascribed to the disordered macromolecular orientation of PET chains and the presence of more voids provided by excessive amounts of SiO_2 nanoparticles acting as stress concentrating defects. During the alkaline hydrolysis, the drop in tensile strength of pure PET fibers is low and slowly decreased. The regression equation

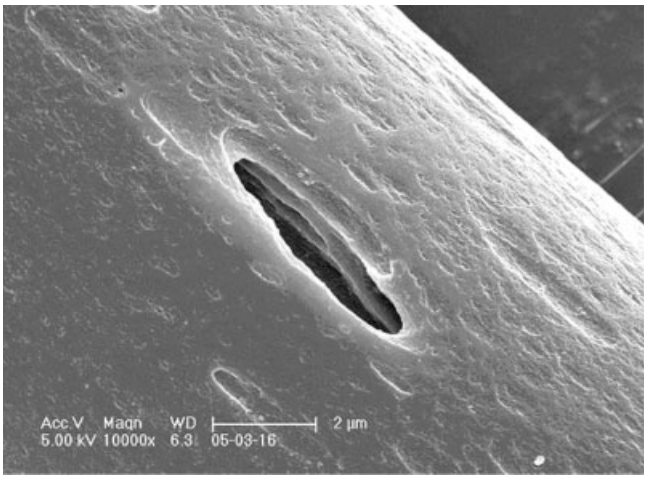

Figure 4 SEM photos of PET/2.0 wt % SiO_2 fiber alkaline hydrolyzed for 10 min.

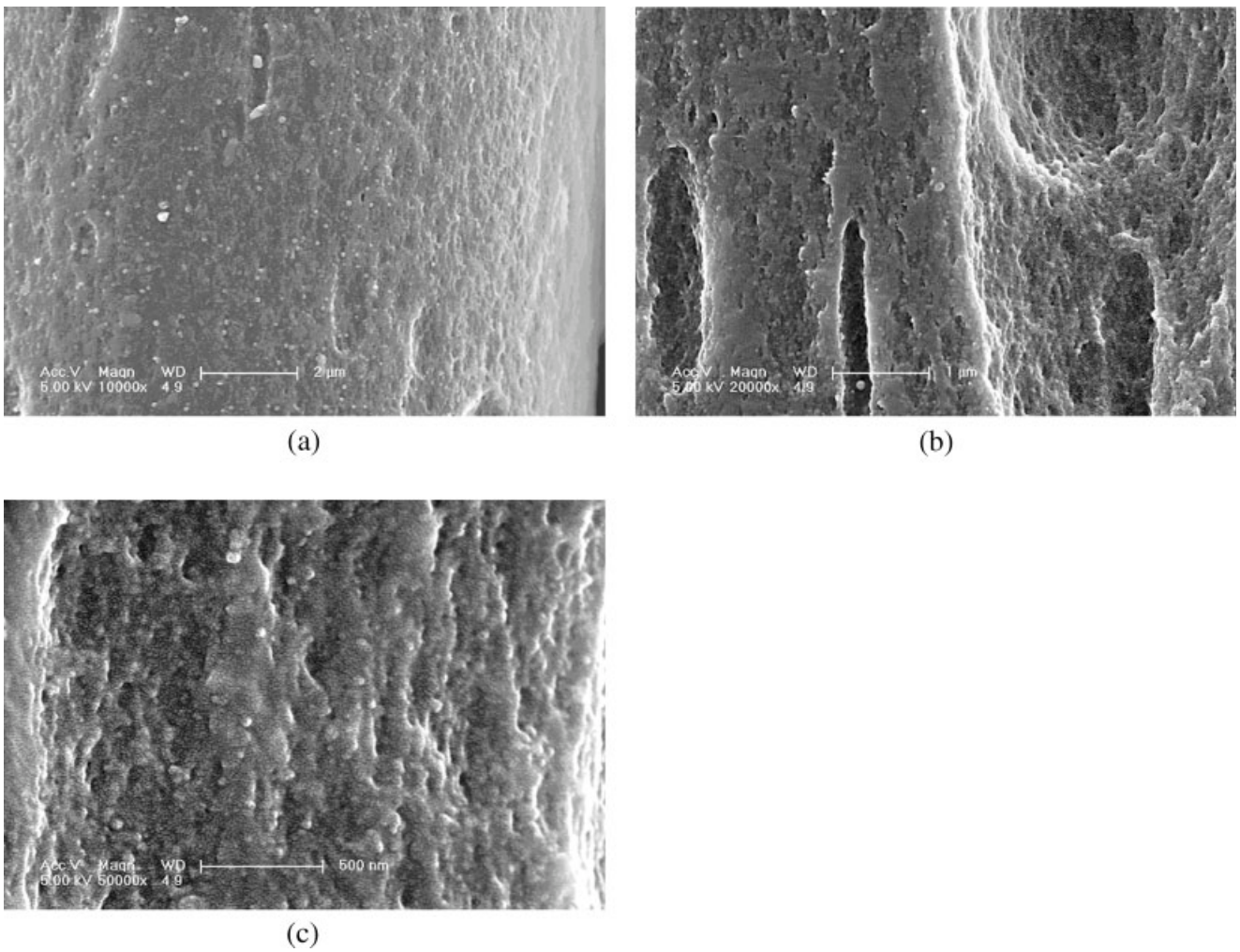

Figure 5 SEM photos of PET/2.0 wt % SiO_2 fiber alkaline hydrolyzed for 30 min.

between tensile strength (S) and alkaline hydrolysis time (T) is of the form $S = 578 - 1.39\ T$. On the other hand, PET/SiO_2 nanocomposite fibers exhibit a drop in tensile strength with WL that is higher for a given time than that of pure PET fibers. The regression equations are of the forms $S = 650 - 2.95\ T$, $S = 570 - 4.12\ T$, $S = 476 - 4.39\ T$ at SiO_2 content of 0.1, 0.5, and 2.0 wt %, respectively. For example, there is a 6.5% decrease in tensile strength for pure PET fibers within 30-min treatment, while its nanocomposite fibers lose 14.9, 20.3, and 30.3%, respectively. This might be due to the formation of more pits on the surface, which probably served as stress concentrating defects when external loads were applied on the fibers. Thus pure PET fibers, with the less pits, show the higher resistance to tensile stress than PET/SiO_2 nanocomposite fibers.

Surface morphologies

To ascertain the extent of damage on the fiber surface in the alkaline hydrolysis, samples were observed using a scanning electron microscope (SEM). SEM photographs in Figure 3 describe the surface morphologies of pure PET fibers hydrolyzed for 30 min. As is well known, the surface of the pure PET fibers without

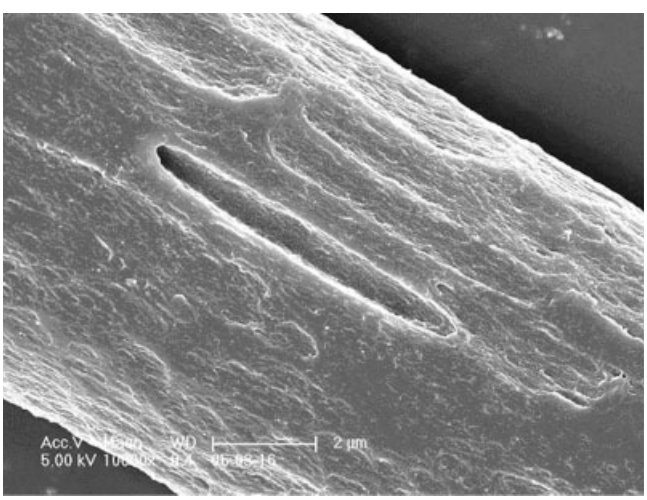

Figure 6 SEM photos of PET/2.0 wt % SiO_2 fiber alkaline hydrolyzed for 60 min.

alkaline hydrolysis was smooth and highly compact. When the fibers were etched in aqueous NaOH, there were some irregular micropits on the surface, which are lengthened along the fibers's axis direction, as shown in Figure 3. In contrast, there are lots of not only micropits but also nanopits in the surface of PET/2.0 wt % SiO_2 fibers, as shown in Figures 4–6. Specific stages in the development of the pits on the hydrolyzed PET/SiO_2 fibers can be recognized. Hydrolysis began at the surface of a PET/SiO_2 nanocomposite fiber and continued until a SiO_2 nanoparticle was exposed (see Fig. 4). Pits appeared to develop from preferential hydrolysis around the SiO_2 nanoparticles, location known to be of lower crystallinity.[6] With continued exposure to NaOH, enlargement of the pits in both depth and length occurred. Hydrolysis over the interior surface area of a pit exposed more and more SiO_2 nanoparticles as polymer degraded around them (see Fig. 5). Finally linkage occurred by advanced erosion of single pits and resulted in merger of adjacent pits (see Fig. 6).

Specific surface area

Knowledge of actual specific surface area may be useful in evaluating the effects of SiO_2 nanoparticles on the microscopic topography of hydrolyzed PET fibers.[31–37] The specific surface areas of hydrolyzed PET fibers are listed in Table III, determined by N_2 adsorption at $-196^{\circ}C$. The specific surface area of the hydrolyzed pure PET fiber is 0.1851 m^2/g, which is similar with previous reported data.[38] As SiO_2 content increases, a substantial increase in specific surface area is observed from 0.1961 to 0.4712 m^2/g for 30-min treatment. This change in specific surface area of fibers is attributed to the more and tougher superfine structure, such as cracks, craters, and cavities shown in Figures 3–6. It is also found that specific surface area generally increased with increasing treatment time. In case of PET/2.0 wt % SiO_2 fiber, specific surface area increases from 0.4212 to 0.9576 m^2/g.

Disperse dye dyeing

Color strength is a term used to describe shade depths of fibers dyed with a disperse dye, which is represented by the K/S value. In this study, measurements of the K/S values of PET fibers can serve as a probe in following fiber structural changes as SiO_2 content changes. The effects of the alkaline hydrolysis time and SiO_2 content on the K/S values of pure PET and PET/SiO_2 fibers are shown in Figure 7. It can be seen that the K/S value of nonhydrolyzed PET fibers increases with increasing SiO_2 content. The difference in K/S values of nonhydrolyzed fibers is mainly ascribed to the presence of SiO_2 nanoparticles, which result in the increase of void spaces necessary for penetration of the disperse dye from the surface into the interior of the fiber.[24,37] These different K/S values could be used to reflect the dye uptake. In contrast, the K/S values of hydrolyzed fibers were also obtained. After alkaline hydrolysis for 20 min, a large number of pits were produced and tough fiber surface formed. The tough surface facilitated the adsorption of disperse dye at the fiber surface and diffused the reflection to a great extent. Consequently, the color shade deepened and the K/S values of all fibers increased. However, the increase in K/S value of PET/SiO_2 nanocomposite fibers after hydrolysis is higher than that of pure PET fibers, which is mainly attributed to the tougher superfine structure, such as such as cracks, craters, and cavities. The increase in K/S value varies in the order pure PET < PET/0.1 wt % SiO_2 < PET/0.5 wt % SiO_2 < PET/2.0 wt % SiO_2. For example, the K/S values of PET/2.0 wt % SiO_2 fibers, hydrolyzed and nonhydrolyzed, are 6.9 and 3.5 K/S larger than those of pure PET fiber.

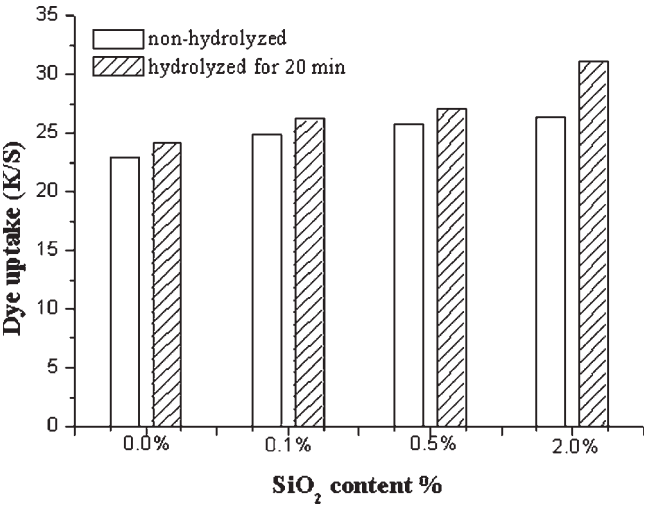

Figure 7 Effect of SiO_2 content on the dye uptake (K/S) value for PET fabrics.

TABLE III
Changes in BET Specific Surface Area of PET/SiO_2 Fibers as a Function of SiO_2 Content and Hydrolysis Time

Sample	Hydrolysis time (min)	BET surface area (m^2/g)
Pure PET	30	0.1851
PET/0.1 wt % SiO_2	30	0.1961
PET/0.5 wt % SiO_2	30	0.3520
PET/2.0 wt % SiO_2	10	0.4212
	30	0.4712
	60	0.9576

CONCLUSIONS

PET/SiO_2 nanocomposites were prepared by *in situ* polymerization and melt-spun to fibers. Differences in the superfine structure and properties between pure PET and PET/SiO_2 fibers were studied. PET/SiO_2

nanocomposite fibers show a greater degree of WL as compared with those of pure PET fibers. More and tougher structure, such as cracks, craters, and cavities, were introduced into the PET/SiO_2 nanocomposite fibers. As a result, alkaline hydrolyzed PET/SiO_2 nanocomposite fibers have the higher specific surface area than pure PET fibers. For the Disperse Blue used, the color strength of the dyeing generally increases with increasing SiO_2 content and alkaline hydrolysis time, owing to the shorter and convenient diffusional path produced by SiO_2 nanoparticles within the PET substrates and the tougher fiber surface. The K/S values of PET/2.0 wt % SiO_2 fibers, hydrolyzed and nonhydrolyzed, are 6.9 and 3.5 K/S larger than those of pure PET fibers.

References

1. Li, Z. M.; Li, L. B.; Shen, K. Z.; Yang, M. B.; Huang, R. Polymer 2005, 46, 5358.
2. Choi, T. S.; Shimizu, Y. Dyes Pigments 2001, 50, 55.
3. Joung, S. N. J Chem Eng Data 1998, 43, 9.
4. Sanches, N. B.; Dias, M. L.; Pacheco, E. B. A. V. Polym Test 2005, 24, 688.
5. Needles, H. L.; Park, M. J. J Appl Polym Sci 1996, 59, 1683.
6. Zeronian, S. H.; Collins, M. J Text Inst 1989, 20, 1.
7. Wei, Z. H.; Gu, Z. Y. J Appl Polym Sci 2001, 81, 1467.
8. Niu, S. H.; Wakida, T.; Ueda, M. Text Res J 1993, 63, 346.
9. Guan, G. H.; Li, C. C.; Zhang, D. J Appl Polym Sci 2005, 95, 1443.
10. Xiao, W. Z.; Yu, H. M.; Han, K. Q.; Yu, M. H. J Appl Polym Sci 2005, 96, 2247.
11. Sanders, E. M.; Zeronian, S. H. J Appl Polym Sci 1982, 27, 4477.
12. Davies, M.; Amirbayat, J. J Text Inst 1994, 85, 376.
13. Niu, S. H.; Wakida, T.; Ueda, M. Text Res J 1992, 62, 575.
14. Gorrofa, A. A. Text Chem Color 1980, 12, 83.
15. Houser, K. D. Text Chem Color 1983, 15, 70.
16. Yamaguchi, S.; Takanable, H. Sen-I Gakkaishi 2001, 57, 111.
17. Solbrig, C. M.; Obendorf, S. K. Text Res J 1991, 61, 177.
18. Collins, M. J; Zeronian, S. H.; Semmelmeyer, M. J Appl Polym Sci 1991, 42, 2149.
19. Kansy, J.; Consolati, G.; Dauwe, C. Phys Chem 2000, 58, 427.
20. Petrovis, Z. S.; Javmi, L.; Waddon, A.; Banhegi, G. J Appl Polym Sci 2000, 76, 2272.
21. Rong, M. Z.; Zhang, M. Q.; Zheng, Y. X.; Zeng, X. M. Polymer 2001, 42, 3301.
22. Tang, Y.; Hu, Y.; Zhang, Z.; Wang, Z. Z.; Gui, Z.; Chen, Z. Y.; Fan, W. C. Macromol Mater Eng 2004, 289, 191.
23. Chan, C. M.; Wu, J. S.; Li, J. X.; Cheung, Y. K. Polymer 2002, 43, 2981.
24. Namboori, C. G. S.; Haith, M. S. J Appl Polym Sci 1999 1968, 12.
25. Betschewa, R.; Wangelov, P. Melliand Textilber 1989, 70, 599.
26. Grancaric, A. M.; Kallay, N. J Appl Polym Sci 1993, 49, 175.
27. Kish, M. H.; Nouri, M. J Appl Polym Sci 1999, 72, 691.
28. Ash, B. J; Siegel, R. W.; Schadler, L. S. J Polym Sci Part B: Polym Phys 2004, 42, 4371.
29. Akpalu, Y. A.; Li, Y.; Siegel, R. W.; Schadler, L. S. J Polym Sci Part B: Polym Phys 2005, 43, 463.
30. Gloaguen, J. M.; Lefebvre, J. M. Polymer 2001, 42, 5841.
31. Liljemark, N. T.; Asnes, H. Text Res J 1971, 41, 732.
32. Ellison, M. S.; Fisher, L. D.; Zeronian, S. H. J Appl Polym Sci 1982, 27, 247.
33. Chatzi, E. G.; Koenig, J. L.; Tidrick, S. L. J Polym Sci 1988, 26, 1585.
34. Ziabicki, A.; Kawai, H. High-Speed Fiber Spinning Science and Engineering Aspects; Wiley: New York, 1985.
35. Huisman, R.; Heuvel, H. M. Ind J Fibre Text Res 1991, 16, 7.
36. Militky, J.; Vanicek, J. Acta Polym 1991, 42, 326.
37. Chen, G. Y.; Cuculo, J. A.; Tucker, P. A. J Appl Polym Sci 1992, 44, 447.
38. Holmes, S. A.; Zeronian, S. H. J Appl Polym Sci 1995, 55, 1573.